



Co-precipitation, impregnation and so-gel preparation of Ni catalysts for pyrolysis-catalytic steam reforming of waste plastics

Dingding Yao^{a,b}, Haiping Yang^{a,*}, Hanping Chen^a, Paul T. Williams^{b,*}

^a State Key Laboratory of Coal Combustion, School of Energy and Power Engineering, Huazhong University of Science and Technology, 430074 Wuhan, China

^b School of Chemical and Process Engineering, University of Leeds, Leeds, LS2 9JT, UK



ARTICLE INFO

Keywords:

Co-precipitation
Sol-gel
Impregnation
Plastic
Hydrogen

ABSTRACT

Three Ni/Al₂O₃ catalysts prepared by co-precipitation, impregnation and sol-gel methods were investigated for the pyrolysis-steam reforming of waste plastics. The influence of Ni loading method on the physicochemical properties and the catalytic activity towards hydrogen and carbon monoxide production were studied. Three different plastic feedstocks were used, high density polyethylene (HDPE), polypropylene (PP) and polystyrene (PS), and compared in relation to syngas production. Results showed that the overall performance of the Ni catalyst prepared by different synthesis method was found to be correlated with the porosity, metal dispersion and the type of coke deposits on the catalyst. The porosity of the catalyst and Ni dispersion were significantly improved using the sol-gel method, producing a catalyst surface area of 305.21 m²/g and average Ni particle size of 15.40 nm, leading to the highest activity among the three catalysts investigated. The least effective catalytic performance was found with the co-precipitation prepared catalyst which was due to the uniform Ni dispersion and the amorphous coke deposits on the catalyst. In regard to the type of plastic, polypropylene experienced more decomposition reactions at the conditions investigated, resulting in higher hydrogen and coke yield. However, the catalytic steam reforming ability was more evident with polystyrene, producing more hydrogen from the feedstock and converting more carbon into carbon monoxide gases. Overall the maximum syngas production was achieved from polystyrene in the presence of the sol-gel prepared Ni/Al₂O₃ catalyst, with production of 62.26 mmol H₂ g⁻¹ plastic and 36.10 mmol CO g⁻¹ plastic.

1. Introduction

World production of waste plastic grows year by year, as a consequence of the huge demand for plastic materials in every commercial field [1]. However, a significant proportion of waste plastics end up into the waste stream leading to many environmental problems. Plastics in the ocean are of increasing concern due to their persistence and effects on the oceans, wildlife and potentially, humans [2]. The cumulative quantity of waste plastic is predicted to be nearly 250 million tonnes per year by 2025. Therefore, there is an urgent need to develop more effective methods to process waste plastics and improve its utilization efficiency.

Chemical recycling processes such as pyrolysis are an effective option to recover energy from waste plastic. A wide distribution of products including gas, chemicals, chars and other products can be obtained from pyrolysis of plastics [3,4]. Furthermore, pyrolysis with a subsequent catalytic steam reforming process enables the conversion of plastic into more valuable gases such as hydrogen [5]. A 60 g/h scale

continuous tank reactor for plastic pyrolysis followed by the catalytic packed-bed reactor for steam reforming was designed by Park [6] and Namioka [7] for the hydrogen-rich gas production from waste polypropylene and polystyrene, while the optimum operating conditions were also studied. Erkiaga et al. [8] compared the products from pyrolysis (500 °C)-steam reforming of HDPE with those from a gasification (900 °C)-steam reforming system by the same authors [9]. Results show that the former one produced a high H₂ yield of 81.5% of the maximum stoichiometric value, which was a little bit lower than the later one (83%) but enabling a more energy-efficient technology for plastics utilization. The pyrolysis and in-line steam reforming of waste plastics has been reviewed by Lopez et al. [10], and they reported that more than 30 wt.% of H₂ yield with up to 70 vol.% of concentration could be obtained.

Catalysts can assist in chain-scission reactions and the breakage of chemical bonds during the pyrolysis-steam reforming process, allowing the decomposition of plastics to occur at a lower temperature and shorten the reaction time. Different types of catalyst such as olivine

* Corresponding authors.

E-mail addresses: yhping2002@163.com (H. Yang), p.t.williams@leeds.ac.uk (P.T. Williams).

[11], Ru [6], Fe [12], and Ni [13,14] catalysts have been investigated for gaseous products from the pyrolysis-reforming of waste plastics. Because of the high activation ability of C–C and C–H bonds on the Ni metal surface as well as the relatively low cost, Ni based catalysts have been a preferred choice in the process [15]. There has been much reported work in the literature devoted to the selection of the optimum loading content, promoters and preparation method of Ni based catalysts for the pyrolysis-reforming of plastics. By varying the flow rate of reduction gas and metal addition to the Ni catalyst, Mazumder et al. [16] found that the acid-base properties, metal dispersion and crystal size of catalyst can be greatly improved. Wu and Williams [17] suggested that the increase in Ni loading could improve hydrogen production from polypropylene, and Mg modified Ni catalyst showed better coke resistance than the non-modified catalysts. Other promoters such as Ce and Zr were also explored, and the improvement in catalyst intrinsic activity was ascribed to the enhancement of water adsorption/dissociation [18]. In order to obtain a higher Ni dispersion, some novel assisted methods were developed to relieve the diffusion resistance of Ni into the inner structure of catalyst. For example, ethylene glycol [19,20] and ethylenediaminetetraacetic acid [21] assisted impregnation methods were used to prepare Ni catalysts with good stability and activity for hydrocarbons reforming.

Catalyst synthesis methods, in particular, the metal loading method, is a curial factor to be considered for catalyst activity. The physical structure and chemical characterizations of the catalyst, including the porosity, reducibility and stability would be closely related to the preparation process [22,23]. Impregnation (or incipient wetness) is the most common method for catalyst preparation, because of the simple procedure and the flexibility to include different catalyst promoters. Co-precipitated Ni catalyst was designed to minimize catalyst deactivation and promote hydrogen production from waste hydrocarbons [24,25]. Meanwhile, sol-gel prepared catalysts have attracted more attention recently [26]. The reinforced impact on Ni dispersion with average size of 20–24 nm was found by using a sol-gel method, leading to superior catalyst activity towards methane reforming [27]. Some reports have compared different catalyst preparation methods, for example, Bibela et al. [28] used a Ni-Ce/Mg-Al catalyst for steam reforming of bio-oil, and found that the wetness impregnated catalyst showed higher carbon conversion than a catalyst prepared via co-precipitation at increasing pH. A sol-gel prepared and promoted Ni/Al₂O₃ catalyst was reported to benefit the metal-support interaction with better particle size uniformity than an impregnated catalyst [27,29]. Around twice the hydrogen yield was produced from steam reforming of ethanol with a Ni/SiO₂ prepared catalyst using a sol-gel method compared with that by an impregnation method [30].

It is known that the co-precipitation, impregnation and sol-gel methods have been adopted as suitable metal loading alternatives for catalyst synthesis. However, the published literatures concerning the comparison of Ni catalyst made by these three methods for catalytic thermal processing of waste plastics are limited. Considering this, the aim of this present work was to investigate Ni/Al₂O₃ catalysts prepared via co-precipitation, impregnation and sol-gel methods for the pyrolysis-steam reforming of waste plastics. The catalyst activity was evaluated in terms of the hydrogen and carbon monoxide production, as well as the catalyst coke formation. In addition, it has been shown that different plastics show different pyrolysis behaviour, producing different product hydrocarbons, which may effect the catalytic steam reforming process and catalyst coke formation and product distributions [31,32]. Therefore, the influence of the type of plastic feedstock on the product selectivity and catalyst activity was also investigated.

This work follows on from our previous reports [4,12,33] which investigated the influence of different types of catalyst and process parameters on the pyrolysis catalytic steam reforming of waste plastics in relation to hydrogen production

Table 1
Ultimate and proximate analysis of different waste plastics.

Waste plastic	Ultimate analysis, wt.%					Proximate analysis ^a , wt.%		
	C	H	O	N	S	Moisture	Volatile	Ash
HDPE	78.18	12.84	3.61	0.06	0.08	0.25	94.77	4.98
PP	83.74	13.71	0.98	0.02	0.08	0.40	98.54	1.06
PS	90.40	8.56	0.18	0.07	0.08	0.20	99.30	0.50

^a Received basis.

2. Experimental

2.1. Feedstock and catalyst preparation

Three different waste plastics, high density polyethylene (HDPE), polypropylene (PP) and polystyrene (PS), which are the most common plastic wastes worldwide, were supplied by Regain Polymers Limited, Castleford, UK. Plastics were collected from real-word waste plastics and mechanically recycled to produce 2–3 mm spheres. The ultimate analysis of the plastic wastes were determined using a Vario Micro Element Analyser, and the results are shown in Table 1. The proximate analyses including moisture, volatiles and ash content of waste plastics were conducted according to ASTM standards E790, E897 and E830, respectively. Briefly, the moisture content was determined by placing 1 g of plastic uniformly in a sample boat in an oven at 105 °C for 1 h. The measurement of volatiles content was operated by using a sealed crucible containing 1 g of plastic in an electric furnace at 950 °C for 7 min, while the ash content was obtained by placing 1 g of plastic in a sample boat in air at 550 °C for 1 h. Results were summarized in Table 1. As the plastics used in this work were from real-world applications instead of the pure polymers, some additives may have been present in the samples. For example, oxygen was detected for the elemental analysis, whereas it would not be present in the pure polymer. Waste HDPE was observed to have the highest ash content of 4.98 wt %, while the other two plastics show little ash content.

The Ni/Al₂O₃ catalysts prepared using co-precipitation method (Ni/Al-Co), impregnation method (Ni/Al-Im) and sol-gel method (Ni/Al-Sg) were tested to catalyse the pyrolysis-reforming of waste plastics. Ni/Al-Im was obtained by a conventional wet impregnation method. 10 g γ-Al₂O₃ and 5.503 g Ni(NO₃)₂·6H₂O (corresponding to Ni loading of 10 wt.%) were mixed in deionized water. The mixture was then stirred using a magnetic stirring apparatus at 100 °C until it turned into slurry. The precursor was dried overnight and calcined at 750 °C for 3 h. The prepared Ni/Al-Co catalyst involved mixing the metallic nitrates of 7.43 g Ni(NO₃)₂·6H₂O and 99.34 g Al(NO₃)₃·9H₂O (Sigma-Aldrich) together with 150 ml deionized water, so that a 10 wt.% Ni loading was obtained. The solution was kept at 40 °C with moderate stirring, then the precursor was precipitated with NH₄(OH) dropwise until the final pH of around 8 was achieved. The precipitates were filtered and washed with deionized water and then dried at 105 °C overnight, followed by calcination at 750 °C in air for 3 h. The Ni/Al-Sg catalyst with the same Ni loading of 10 wt.% was prepared by a simple sol-gel method. 20 g of Aluminium tri-sec-butoxide (ATB, Sigma-Aldrich, 97%) was firstly dissolved into 150 ml absolute ethanol (> 99.5%, Merck) and stirred for 2.5 h at 50 °C. 2.210 g of Ni(NO₃)₂·6H₂O was dissolved in 8 ml deionised water separately to form the Ni precursor. Then the Ni solution was pipetted into the support solution while maintaining stirring at 75 °C for 0.5 h. 1 M HNO₃ was added into above solution until the pH of 4.8 was obtained. After drying at 105 °C overnight, the precursors were calcined at 450 °C in air for 3 h.

All of the catalysts were ground and sieved with a size range between 50 and 212 μm. The catalysts used in this work were reduced in 5 vol.% H₂ (balanced with N₂) atmosphere at 800 °C for 1 h before each experiment.

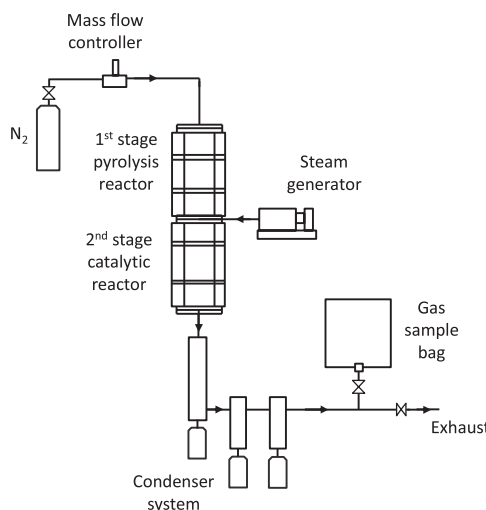


Fig. 1. Schematic diagram of the pyrolysis-reforming of waste plastics system.

2.2. Catalyst testing for plastic gasification

A schematic diagram of the pyrolysis-catalytic steam reforming reactor system for waste plastics is shown in Fig. 1 [33]. The experimental system consisted essentially of a continuous steam injection system using a water syringe pump, a nitrogen gas supply system, a two-stage stainless tube reactor, a gaseous product condensing system using dry ice, and gas measurement system. The reactor has two separate heating zones, i.e. first stage plastic pyrolysis reactor of 200 mm height and 40 mm i.d; second stage catalytic reactor of 300 mm height and 22 mm i.d. The real temperatures of two zones were monitored by thermocouples placing in the middle of each reactor and controlled separately. The calibration of the reactor temperature was performed before this set of experiments, and the temperature described in this paper was given as the real one. For each experiment, 0.5 g of catalyst was loaded into the second stage where the temperature was maintained at 800 °C. High purity nitrogen was supplied as the inert carrier gas. 1 g of plastics were placed in the first stage and then heated from room temperature to 500 °C at 40 °C min⁻¹, and the evolved volatiles passed into the catalyst reactor for reforming. Water was injected into the second stage with a flow rate of 6 g h⁻¹. After the reforming process, the condensable liquids were collected into condensers while the non-condensable gases were collected into a 251 Tedlar™ gas sample bag off-line gas chromatography (GC) measurement. Each experiment was repeated to ensure the reliability of the results.

2.3. Product analysis

The gas products were separated and quantified by packed column GCs. A Varian 3380 GC packed with 60–80 mesh molecular sieve, coupled with thermal conductivity detector (TCD) was used to analyse permanent gases (H₂, O₂, N₂, CO). CO₂ was determined by another Varian 3380 GC/TCD. Argon was used as the carrier gas for both GCs. Hydrocarbons (C₁ to C₄) were analysed using a different Varian 3380 GC/FID coupled with a HayeSep 80–100 mesh molecular sieve column and using nitrogen as carrier gas. Each gas compound mass yield was calculated combining the flow rate of nitrogen and its composition obtained from the GC.

The yield of non-reacted pyrolysis oil was calculated as the mass difference between fresh and used condenser system in relation to the total weight of plastic and steam input. Coke yield was determined from the temperature programmed oxidation analysis of the spent catalyst. Residue yield was measured as the mass difference between fresh and the used whole reactor system in relation to the total weight of plastic and steam input. Mass balance was therefore calculated as the sum of

gas, liquid and residue obtained in relation to the total plastic and steam input.

2.4. Catalyst characterisation

X-ray diffraction (XRD) analysis of the fresh catalysts was carried out using a Bruker D8 instrument with Cu K α radiation operated at 40 kV and 40 mA. In order to explore the distribution of active sites on the catalysts, the Debye-Scherrer equation was used to obtain the average crystal size from the XRD results. The porous properties of the fresh catalysts were determined using a Nova 2200e instrument. Around 0.2 g of each sample was degassed at 300 °C for 2 h prior to the analysis. The specific surface area was calculated using Brunauer, Emmett and Teller (BET) method. The total pore volume was determined at a relative pressure P/P₀ of 0.99, and the pore distribution was obtained from the desorption isotherms via the BJH method. In order to determine the actual loading of nickel in the catalyst, a Optima 5300DV (Perkin Elmer Inc.) inductively coupled plasma optical emission spectrometer(ICP-OES)was used. About 25 mg of catalyst was previously dissolved in acidic solution, followed by diluting with deionized water to 50 ml in preparation for analysis.

The morphologies of the fresh prepared catalysts and the coke deposited on the used catalysts were investigated using a Hitachi SU8230 scanning electron microscope (SEM), which was operated at 2 kV and working distance of 3 mm. An energy dispersive X-ray spectroscope (EDXS) was connected to the SEM to study the elemental distribution. A FEI Helios G4 CX Dual Beam SEM with precise focused ion beam (FIB) was used to analyse the cross-section of the prepared catalysts. Before the analysis, the catalyst was coated with platinum in order to protect the sample during the sectioning process. Fresh catalysts were further examined at a higher magnification by a high-resolution transmission electron microscope (TEM, FEI Tecnai TF20) coupled with a connected EDXS for microstructure and elemental distribution. For the TEM analysis preparation, samples were initially dispersed well in methanol using an ultrasonic apparatus, and were pipetted on to a carbon film coated copper grid. The coke deposited on the surface of catalyst was characterized by temperature programmed oxidation (TPO) with a Shimadzu TGA 50. For each TPO analysis, around 25 mg of spent catalyst was heated from room temperature to 800 °C in an air atmosphere (100 ml min⁻¹) at a heating rate of 15 °C min⁻¹ and a holding time of 10 min at 800 °C.

3. Results

3.1. Characterization of fresh catalyst

The XRD patterns of the fresh catalysts are shown in Fig. 2. The Ni/Al₂O₃ catalyst prepared by the impregnation method produced sharp peaks compared to the other fresh catalysts. The easily identified peaks centred at 2θ = 44.5, 51.9 and 76.4° corresponding to the (111), (200) and (220) plane respectively, confirmed the presence of Ni (JCPDS: 01-087-0712) in the cubic form. The aluminium oxides at 37.6, 45.8, 66.8° were also determined (00-029-0063). As there was no NiO detected from the XRD results, it demonstrates that the nickel catalyst precursors had been completely reduced into active compounds (Ni) before each experiment. According to the Scherrer equation, the average crystallite size of Ni based on the main peak at around 2θ at 44.5° was determined to be 26.17, 52.28 and 19.69 nm for the Ni/Al-Co, Ni/Al-Im and Ni/Al-Sg catalysts, respectively. This indicates that a higher Ni dispersion and smaller Ni particles were found for the catalyst prepared by the sol-gel method compared with impregnation and co-precipitation.

Table 2 summarizes the BET surface areas and pore size properties of the fresh nickel Ni/Al₂O₃ catalysts. The Ni/Al-Co and Ni/Al-Im catalyst showed surface areas of 192.24 and 146.41 m² g⁻¹, respectively. The Ni catalyst produced via the sol-gel method showed a higher surface area of 305.21 m² g⁻¹ compared to the catalysts obtained by

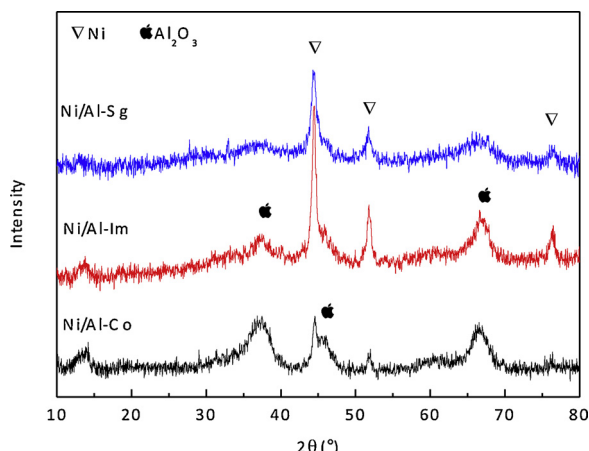


Fig. 2. XRD analysis of fresh Ni/Al catalysts.

Table 2
Properties of different fresh Ni/Al catalysts.

	Porosity analysis		ICP-OES analysis		
	Surface area ^a (m ² /g)	Pore volume ^b (ml/g)	Average pore size ^c (nm)	Ni loading (wt.%)	Standard deviation
Ni/Al-Co	192.24	0.404	6.642	8.04	1.00
Ni/Al-Im	146.41	0.387	6.594	10.05	1.30
Ni/Al-Sg	305.21	0.915	6.642	8.50	0.84

^a Determined by BET method.

^b Determined from BJH desorption pore volume.

^c Determined from BJH desorption average pore diameter.

impregnation or co-precipitation. The Ni/Al-Sg catalyst also gave the highest pore volume of 0.915 ml g^{-1} while Ni/Al-Im generated the lowest. However, the average pore size of these three catalysts were similar, at around 6.6 nm. Therefore, it indicates that the Ni catalyst prepared by the sol-gel method gives a more porous structure compared

to the other two methods. The adsorption/desorption isotherms and pore size distribution of fresh catalysts are shown in Fig. 3. All of the physisorption isotherm types for the three catalysts appear to be type IV according to the IUPAC classification [34]. From the pore size distributions, the Ni/Al₂O₃ catalyst prepared by the sol-gel method shows a quite narrow pore size distribution, while the impregnated prepared catalyst shows a broad distribution. This indicates that compared with Ni/Al-Co and Ni/Al-Im catalyst, the Ni/Al-Sg catalyst produces a more uniform porous structure, and most pores are with a size of around 6.64 nm. Therefore, it may be concluded that a mesostructured Ni/Al₂O₃ catalyst can be obtained by the sol-gel preparation method. The results of the real nickel loading from ICP-OES analysis was also listed in Table 2. It can be seen the real content of Ni in the co-precipitated and sol-gel catalyst was a little lower than the designed value, while it was excellent agreement for the impregnated Ni/Al-Im catalyst. In summary, the active Ni sites were successfully loaded into the catalyst by different preparation method.

The morphologies and the distribution of active metallic Ni for the fresh catalysts were determined by SEM-EDX analysis, as shown in Fig. 4. Compared with the Ni/Al-Co catalyst shown in Fig. 4, which shows a flat surface, the catalyst particles of Ni/Al-Im observed were irregular. The nickel catalyst prepared by the sol-gel method seems to be composed of many small particles in a loose structure. The Ni EDX mapping showed a uniform distribution of Ni particles in the catalysts. In order to investigate the inner structure of the fresh catalysts, the cross-sectional morphologies of catalyst particles were examined by FIB/SEM. From Fig. 5, the Ni/Al-Co catalyst which has a relatively low surface area (Table 2) shows a tight structure, whereas the Ni/Al-Sg catalyst shows a porous inner structure. The observations agree well with the porosity results that show the Ni/Al-Sg catalyst generates a higher surface area and higher pore volume compared with the other catalysts. This type of structure was reported to benefit Ni penetration inside the catalyst particles, and further promote the catalyst activity [33].

The fresh catalysts were further examined under high magnification by TEM and the results are shown in Fig. 6. The images show obvious dark spots, which were ascribed to the presence of metallic Ni. As can be seen, all the Ni particles were well dispersed, and hardly any

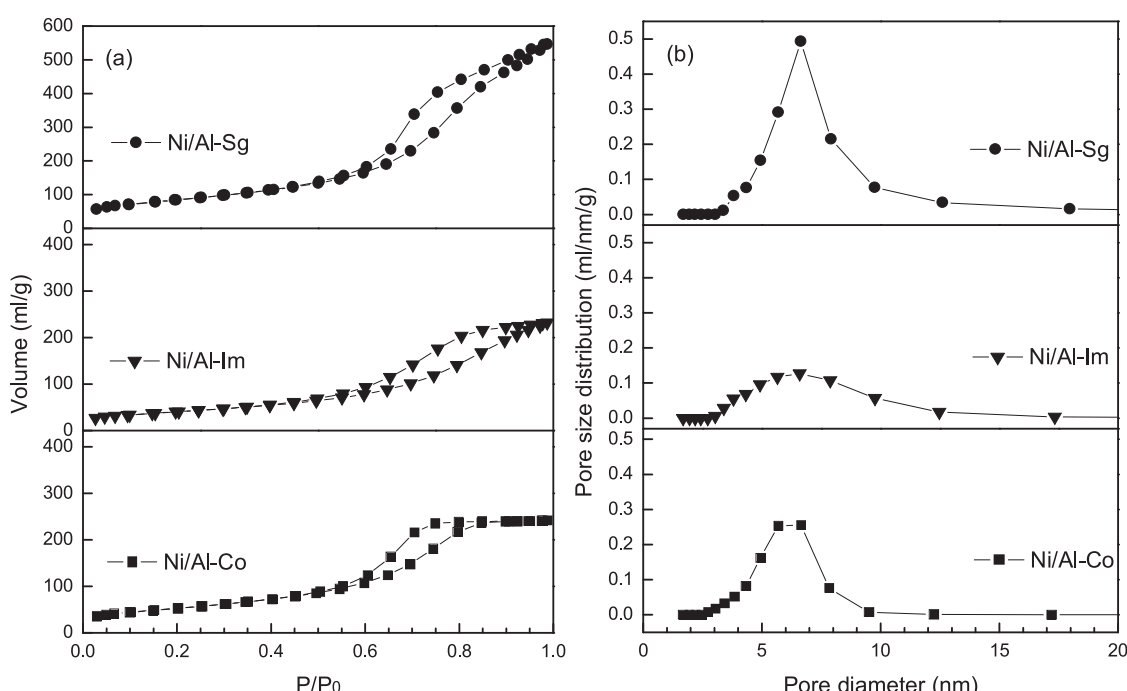


Fig. 3. Adsorption/desorption isotherm (a) and pore size distributions (b) of fresh Ni/Al catalysts.

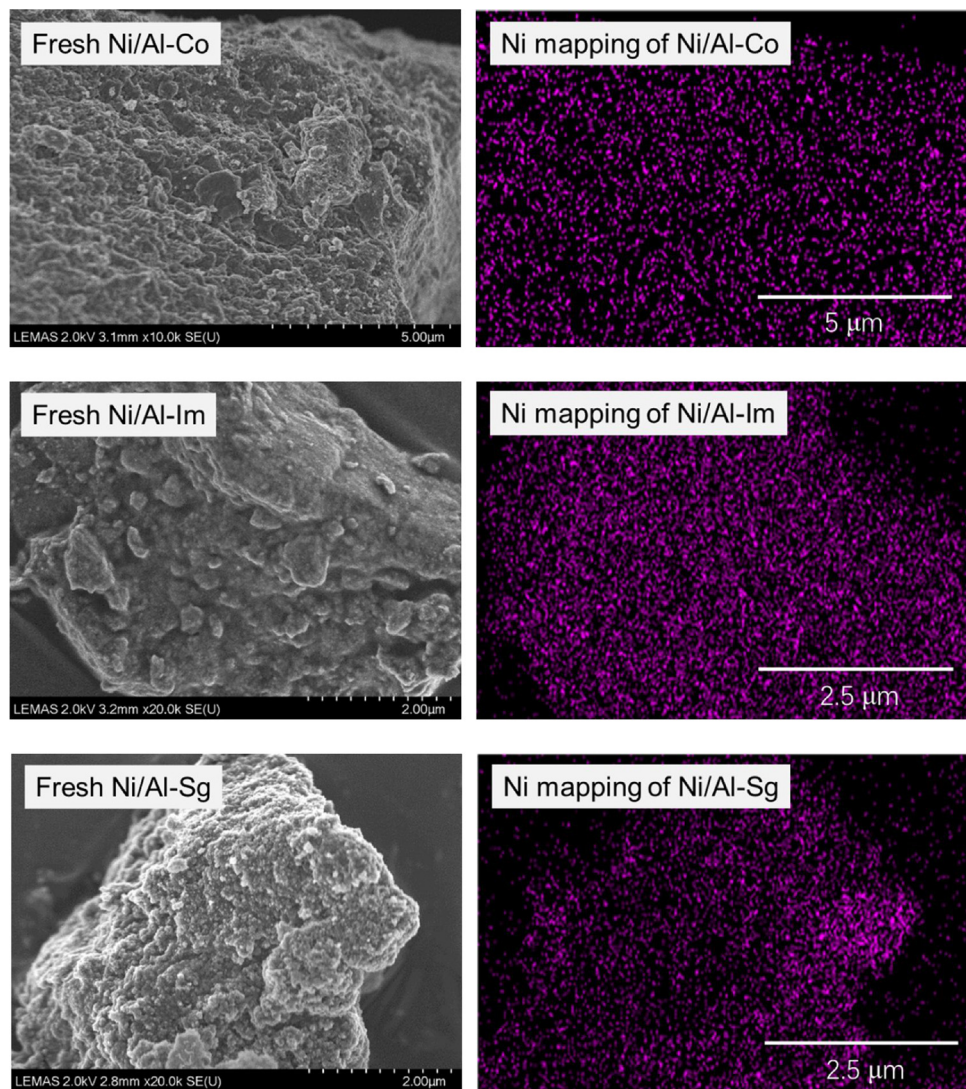


Fig. 4. The morphologies of fresh catalysts. SEM and Ni mapping of Ni/Al-Co, Ni/Al-Im and Ni/Al-Sg.

agglomeration was seen. Statistical analysis of the Ni particle size distributions of the three TEM images was carried out by ImageJ software, and the results are shown in Fig. 6(d)–(f). More than 95 percent of the Ni particles present were of a size less than 50 nm. The Ni/Al catalyst prepared by the sol-gel method showed the narrowest size distribution, with the smallest average particle size of 15.40 nm. Both Ni/Al-Co and Ni/Al-Im catalysts have a size distribution concentrated at 15~30 nm, but they show larger average particle size of 28.91 and 29.60 nm, respectively. Therefore, the sol-gel prepared catalyst exhibited the highest homogeneity and smallest active metal size among the three catalysts, which is in good agreement with the results from XRD analysis. The EDX mappings of the sol-gel synthesized Ni/Al catalyst shown in Fig. 6(g) also demonstrate that both the Ni and Al were uniformly distributed inside the catalyst.

3.2. Catalyst investigation for catalytic reforming of waste polyethylene (HDPE)

The use of different nickel catalysts prepared via co-precipitation, impregnation and sol-gel methods for the pyrolysis-catalytic steam reforming of waste polyethylene was investigated in this section. The results of syngas production and gas composition are summarized in Table 3. The mass balance of all the experiments in this paper were calculated to be in the range of 92 to 98 wt.%. In addition, results from

the repeated trials show that the standard deviations of the hydrogen and carbon monoxide yield were 0.26 and 0.29 mmol g⁻¹ plastic respectively. For the volumetric gas concentrations, the standard deviation was 0.26% for H₂ and 0.08% for CO respectively. These data indicates the reliability of the experimental procedure. From Table 3, the highest hydrogen yield of 60.26 mmol g⁻¹ plastic was obtained with the Ni/Al catalyst prepared by the sol-gel method, followed by that prepared by the impregnation method. The lowest hydrogen yield of 43.07 mmol g⁻¹ plastic was obtained with the Ni/Al-Co catalyst. The production of carbon monoxide has the same trend as that of hydrogen yield. Syngas production achieved its maximum with the Ni/Al-Sg catalyst, that is, per unit mass of the polyethylene can yield 83.28 mmol of syngas. The gas composition is also shown in Table 3. It can be observed that the concentration of H₂ and CO₂ were steadily increased with the catalyst order: Ni/Al-Co < Ni/Al-Im < Ni/Al-Sg, while the content of CH₄, CO and C₂–C₄ were decreased correspondingly. During the pyrolysis-reforming of waste plastic, the thermal decomposition of plastic occurs in the pyrolysis stage as Eq. (1). The pyrolysis volatiles were then steam reformed by the catalyst to produce more valuable gases like hydrogen and carbon monoxide (Eqs. (2) and (3)). As the CH₄ and C₂–C₄ concentrations from Ni/Al-Sg were rather lower, while H₂ and CO yields were significantly higher than those from the other two catalysts, it can be concluded that the steam reforming of hydrocarbons (Eq. (2)) was greatly promoted in the presence of the Ni/Al-Sg catalyst. In addition,

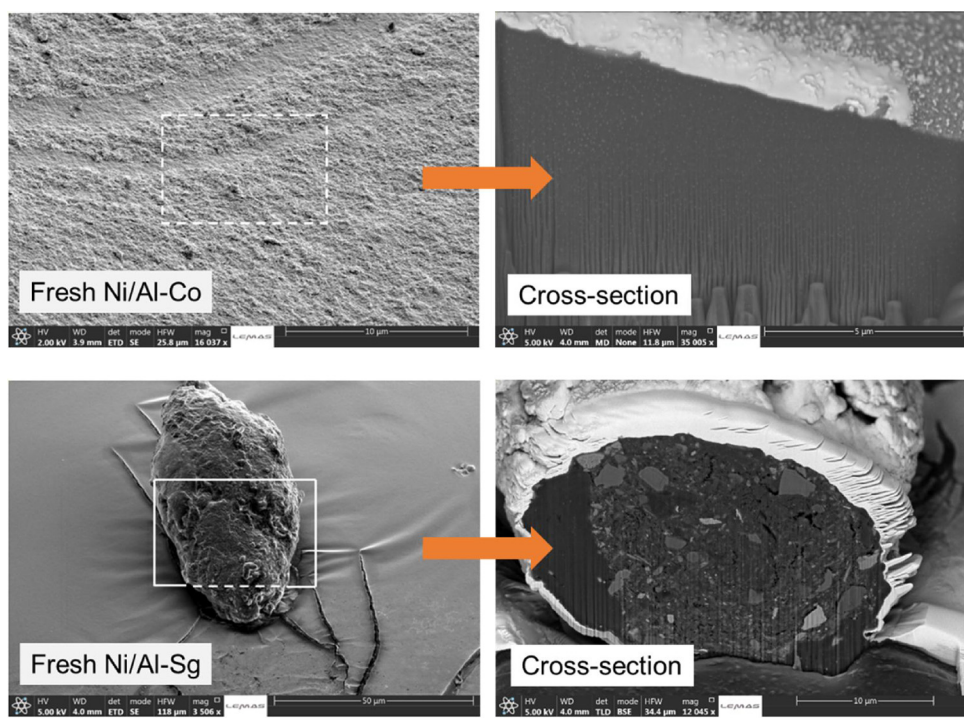


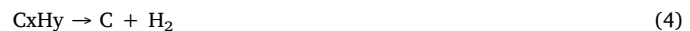
Fig. 5. FIM-SEM analysis of Ni/Al-Co and Ni/Al-Sg.

the ratio of H₂ to CO, which can reveal the degree of waster gas shift reaction Eq. (3), achieved its maximum of 2.62 with the Ni/Al-Sg catalyst. Therefore, the nickel catalyst prepared by sol-gel method displayed the highest activity to both hydrocarbons reforming and water gas shift reactions among the three catalysts investigated.



Temperature programmed oxidation was used to investigate the coke deposition on the used catalyst. As shown in Fig. 7, the oxidation process involved three main stages: the removal of water in the range of 100 ~ 300 °C, the oxidation of Ni from 300 to 450 °C, and carbonaceous coke combustion from 450 °C onwards, which were also observed in our previous studies [35]. The amount of coke was calculated based on the weight loss of spent catalyst from 450 °C (when Ni had finished oxidation and coke started to combust) to 800 °C, and the results are shown in Table 3. It can be observed that, during the pyrolysis-catalytic steam reforming of waste polyethylene, the Ni/Al-Sg catalyst produced the highest coke yield of 7.41 wt.% among the three catalysts, but displayed the highest catalyst activity for syngas production. In addition, the Ni/Al-Co catalyst which generated the lowest hydrogen yield produced the least coke formation. It should be noted that the catalytic volatiles thermal cracking Eq. (4) may also be involved during this process. The results regarding syngas production and coke yield with the three catalysts indicate that the Ni/Al-Sg catalyst showed high catalytic activity for both reforming reactions and volatiles thermal cracking reactions. The derivative weight loss thermograms in Fig. 7 showed two distinct peaks at temperatures around 530 and 650 °C. It has been reported that the oxidation peak at lower temperature was related to amorphous coke, while the peak at higher temperature is linked to graphitic filamentous coke oxidation [12,36]. The coke deposited on the Ni/Al-Sg catalyst appears to be mainly in the form of filamentous carbon, which was also confirmed in the SEM morphology analysis shown in Fig. 8(c). While for the Ni/Al-Co catalyst SEM results shown in Fig. 8(a), more coke deposits without any regular shapes were observed. The larger

production of amorphous coke on the spent Ni/Al-Co catalyst compared with the other two catalysts could also be responsible for the lower syngas production, since the amorphous coke was considered to be more detrimental to catalyst activity than the filamentous carbons. In addition, compared with the SEM results of the fresh catalysts shown in Fig. 4, the morphologies of the three nickel catalysts did not change significantly. For example, the catalyst prepared by the sol-gel method, maintained its loose structure after the reforming process, indicating the good thermal stability of the catalyst.



3.3. Catalyst investigation for catalytic reforming of waste polypropylene (PP)

Polypropylene was also investigated for the pyrolysis-catalytic steam reforming process for hydrogen production in the presence of the three different Ni/Al catalysts to produce more gases. The gas productions and concentrations are shown in Table 4. The Ni/Al-Sg catalyst displayed the most efficient catalytic activity in terms of the steam reforming of the polypropylene, as the gas yield was 144.03 wt.% which was much higher than the other two catalysts. In addition, much higher hydrogen yield (67.00 mmol g⁻¹_{plastic}) and carbon monoxide yield (29.98 mmol g⁻¹_{plastic}) were obtained by using the Ni/Al-Sg catalyst. The syngas production from PP with the Ni/Al-Sg catalyst was slightly higher than was observed from HDPE, and this phenomenon can also be found with the Ni/Al-Co and Ni/Al-Im catalysts. This may be due to the higher hydrogen and carbon content and lower ash content of PP compared with HDPE (Table 1), and which suggests more effective hydrocarbons participation in the reforming reactions to obtain more syngas. The nickel catalyst prepared by the co-precipitation method showed the least activity for the reforming process, producing 46.05 mmol H₂ g⁻¹_{plastic} and 20.39 mmol CO g⁻¹_{plastic}. The composition of the gases from waste polypropylene were mainly composed of H₂, CH₄, CO, C₂₋₄ hydrocarbons and CO₂. The concentration of H₂ and CO with Ni/Al-Sg achieved 59.38 and 26.57 vol.%, respectively. The CH₄ and C₂₋₄ gases content with the Ni/Al-Sg catalyst were lower than the case

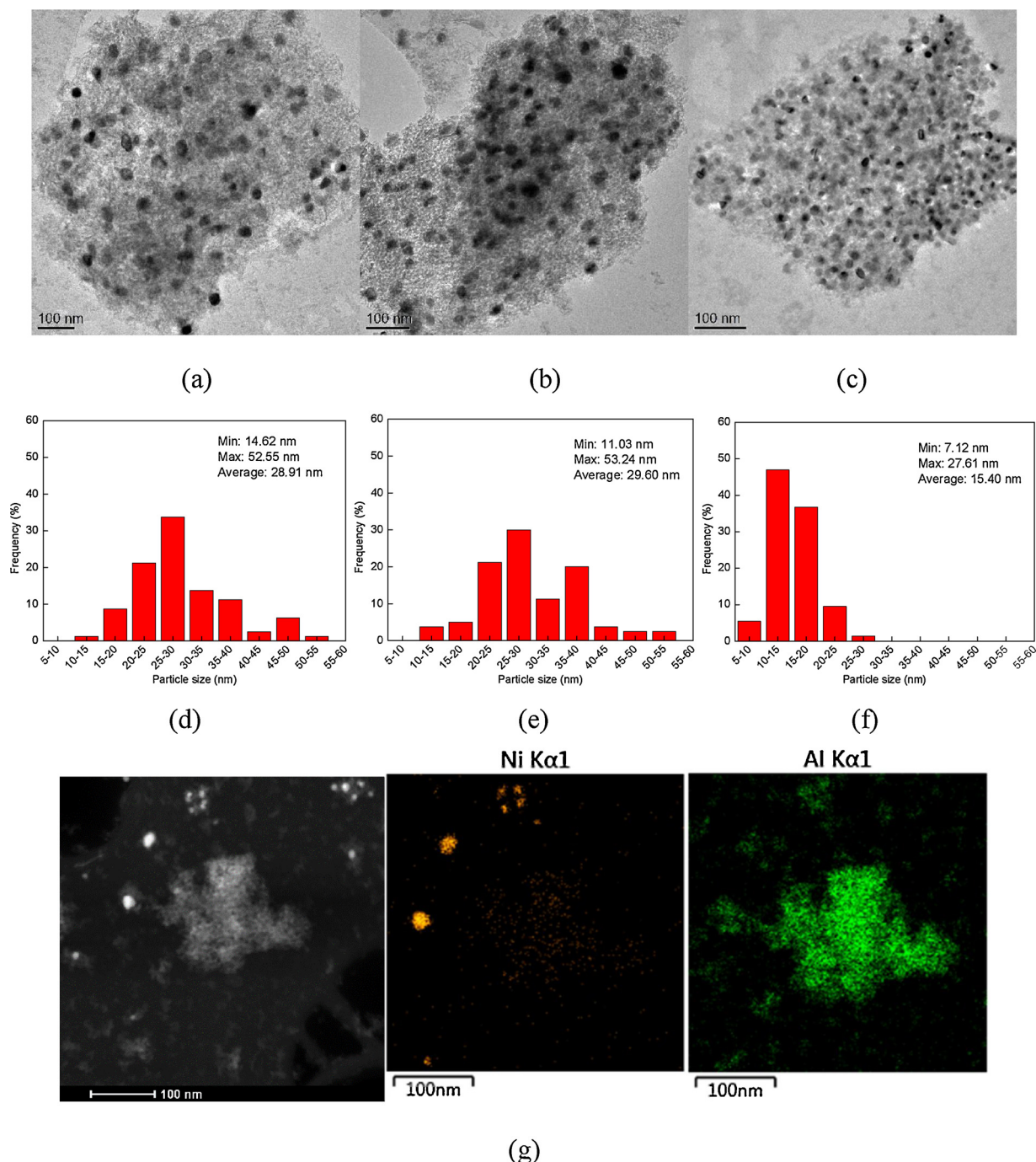


Fig. 6. TEM analysis of fresh (a) Ni/Al-Co, (b) Ni/Al-Im (c) Ni/Al-Sg catalyst, and (d)–(f) the corresponding Ni particle distribution, and (g) Ni and Al mapping of fresh Ni/Al-Sg catalyst by EDX analysis.

with the other two catalysts, which also indicates the higher catalytic activity of the catalyst made by the sol-gel method.

The amount and the type of coke deposition on the three catalysts from the pyrolysis-steam reforming of polypropylene were determined by TPO analysis, as shown in Fig. 9. The amount of carbonaceous coke was calculated and the results are shown in Table 4. The Ni/Al-Co and Ni/Al-Im catalysts produced around 5 to 6 wt.% of coke, lower than the case of the Ni/Al-Sg catalyst which showed a 8.49 wt.% coke yield. From the derivative weight loss results, the peak associated with amorphous carbon was much larger than that of the filamentous carbon with the Ni/Al-Co catalyst. However, for the Ni/Al-Im and Ni/Al-Sg catalysts, produced more filamentous carbons. This phenomenon was also observed with HDPE. It can be deduced that the nickel catalyst

prepared by impregnation and sol-gel methods favour the production of filamentous carbonaceous coke from the pyrolysis-steam reforming of waste plastics. The presence of both amorphous carbon and filamentous carbon with the Ni/Al-Co and Ni/Al-Im catalyst were further confirmed by the SEM images shown in Fig. 10(a) and (b). Fig. 10(c) shows that the deposits on the used Ni/Al-Sg catalyst were predominantly filamentous carbon. Furthermore, there was a dense covering of carbon on the catalyst no matter which type of catalyst was used. The amount of carbon deposits from SEM images seems to be larger for PP than the case for HDPE, which was consistent with the TPO results.

Wu and Williams [13] used an incipient wetness method (similar to the impregnation method in this work) prepared Ni/Al₂O₃ for steam gasification of PP. A potential H₂ yield of 26.7 wt.% was obtained, with

Table 3

Gas productions from pyrolysis-catalytic steam reforming of waste polyethylene.

	Ni/Al-Co	Ni/Al-Im	Ni/Al-Sg
H ₂ yield, mmol g _{plastic} ⁻¹	43.07	51.51	60.26
CO yield, mmol g _{plastic} ⁻¹	18.27	21.51	23.02
Syngas yield, mmol g _{plastic} ⁻¹	61.34	73.01	83.28
Gas yield in relation to plastic only, wt.%	93.38	109.77	119.76
Coke yield in relation to plastic only, wt.%	2.92	3.80	7.41
Gas composition, vol.%			
H ₂	58.68	59.24	61.99
CH ₄	6.91	6.68	5.43
CO	24.88	24.73	23.68
CO ₂	4.51	4.80	6.62
C ₂ -C ₄	5.02	4.55	2.29
H ₂ /CO ratio	2.36	2.60	2.62
Gas yield in relation to plastic & steam, wt.%	24.86	27.44	29.94
Liquid yield in relation to plastic & steam, wt.%	66.04	64.20	59.87
Residue in relation to plastic & steam, wt.%	1.62	1.98	2.43
Mass balance, wt.%	92.52	93.62	92.24

the gaseous product containing 56.3 vol.% of H₂ and 20.0 vol.% of CO. The syngas production can be calculated as 77.62 mmol g_{plastic}⁻¹, which was close to the yield obtained in this study (75.77 mmol g_{plastic}⁻¹). However, the coke deposition (11.2 wt.%) was higher than from this study (5.34 wt.%), which might be due to the lower surface area (90 m²/g) compared with Ni/Al-Im used here (146.41 m²/g). High hydrogen yields of 21.9 g g_{PP}⁻¹ and 52 wt.% (potential value) were obtained by the same authors from polypropylene with co-precipitation prepared Ni-Mg-Al (Ni:Mg:Al ratio = 1:1:1, 800 °C, 4.74 g h⁻¹ steam) [37] and co-impregnated Ni/CeO₂/Al₂O₃ catalyst (Ni 10 wt.%, CeO₂ 20 wt.%, 900 °C) [14], respectively. It should be noted that the Ni catalysts in these literatures were prepared either at a higher loading or with promoter added, otherwise using at higher catalysis temperature. It also suggests that hydrogen production can be promoted by the use of effective catalyst promoters or by regulation of operational parameters. Czernik and French [38] concluded that many common plastics can be converted into hydrogen by thermo-catalytic process with a microscale reactor interfaced with molecular beam mass spectrometer. A bench-scale plastic pyrolysis-reforming system was also carried out by them using PP as a representative polymer, while 20.5 g/h H₂ was generated with a 60 g/h of PP feeding rate.

3.4. Catalyst investigation for catalytic reforming of waste polystyrene (PS)

The product distributions in terms of gas yield and composition from the pyrolysis-catalytic steam reforming of waste polystyrene with the different catalysts are displayed in Table 5. The Ni/Al-Co catalyst

produced a H₂ yield of 51.31 mmol g_{plastic}⁻¹ which was a little lower than the yield of 55.04 mmol H₂ g_{plastic}⁻¹ with the Ni/Al-Im catalyst. Among the three catalysts, the Ni/Al-Sg catalyst produced the maximum H₂ yield and CO yield per mass of plastic feedstock, which was also observed with HDPE and PP. However, compared with HDPE and PP, PS shows a comparatively higher yield of CO, with values up to 36.10 mmol g_{plastic}⁻¹ with the sol-gel prepared catalyst. Most of the concentrations of CO and CO₂ obtained from PS were also larger than the corresponding data from PP or HDPE. It may due to the higher content of elemental carbon in the feedstock. In addition, as the coke yield produced using PS was lower than from PP or HDPE except from those with Ni/Al-Co, it suggests most of the carbon in PS was converted into gas product by participating in catalytic steam reforming reactions Eq. (2) or the water gas shift reaction Eq. (3). The hydrogen content of the product gases fluctuated slightly in the range of 57.90 and 59.32 vol.% depending on the different catalyst applied. The hydrocarbons in the final gas product were relatively low for PS whichever type of catalyst was used, and the concentration of C₂-C₄ was less than 1.10 vol.%. The water gas shift reaction Eq. (3) was promoted by the Ni/Al-Co catalyst as the H₂/CO ratio was higher than with the other catalysts.

TPO analysis of the used catalysts from the pyrolysis-catalytic steam reforming of polystyrene was also carried out to characterize the carbonaceous coke deposition on the catalyst, as shown in Fig. 11. The results of the calculated amount of coke produced are shown in Table 5. The Ni/Al-Sg catalyst produced the highest coke yield of 6.14 wt.% even though it produced the largest hydrogen production amongst the three catalysts. It suggests that both steam reforming and decomposition of hydrocarbons Eq. (3) and Eq. (4) were significantly facilitated with the Ni/Al-Sg catalyst during the pyrolysis-steam reforming of waste polystyrene. As for the type of carbon deposits, overlapping derivative weight loss peaks were observed with the Ni/Al-Im and Ni/Al-Sg catalysts, indicating that both amorphous and filamentous coke were produced. This is in agreement with the morphologies observed by SEM images shown in Fig. 12. The Ni/Al catalyst prepared by co-precipitation displayed the deposits in a great proportion of amorphous form, and the derivative TPO peak at lower temperature was more significant than that at higher oxidation temperature.

4. Discussion

4.1. Effect of the preparation method of catalyst on syngas production and coke deposits

The yield of hydrogen and carbon monoxide from pyrolysis-steam reforming of waste plastics varied with the catalyst preparation method used. Overall, despite the difference in the feedstock, the sol-gel

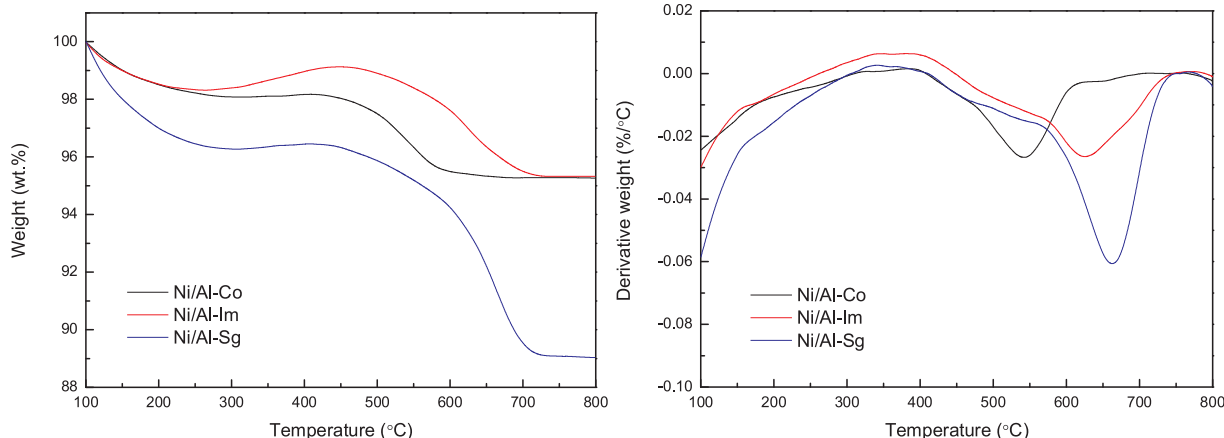


Fig. 7. Temperature programmed oxidation of reacted Ni/Al catalysts for waste polyethylene.

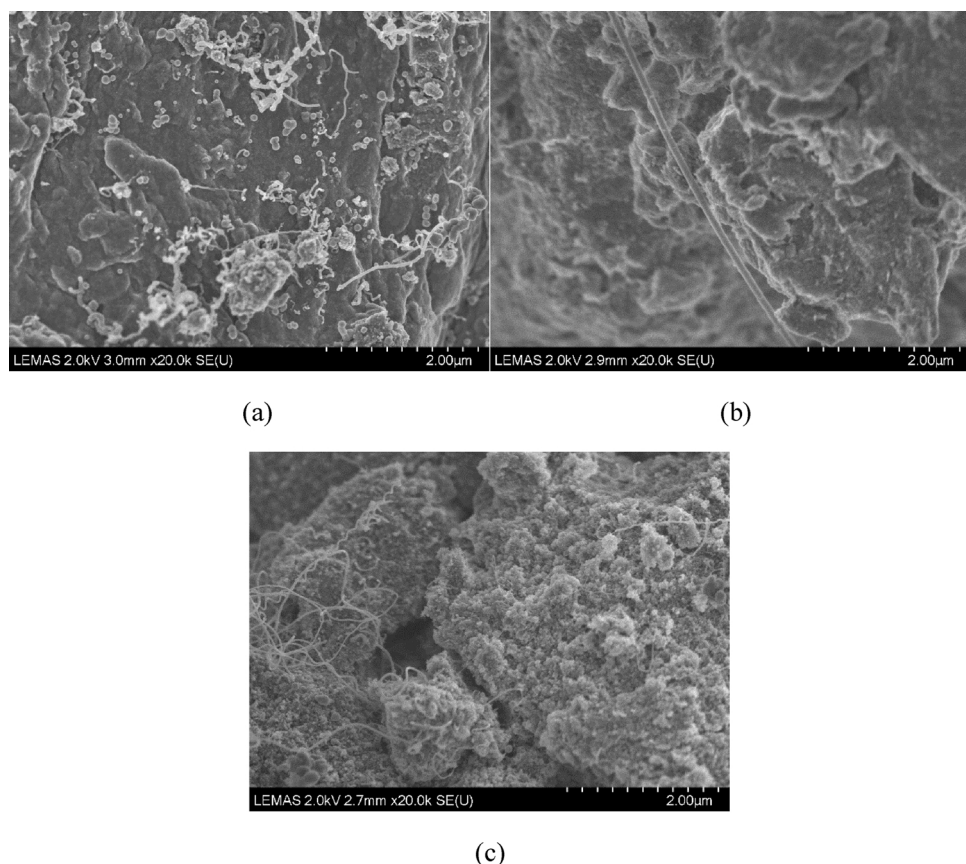


Fig. 8. SEM images of reacted (a) Ni/Al-Co, (b) Ni/Al-Im and (c) Ni/Al-Sg catalyst from waste polyethylene.

Table 4

Gas productions from pyrolysis-catalytic steam reforming of waste polypropylene.

	Ni/Al-Co	Ni/Al-Im	Ni/Al-Sg
H ₂ yield, mmol g _{plastic} ⁻¹	46.05	52.06	67.00
CO yield, mmol g _{plastic} ⁻¹	20.39	23.71	29.98
Syngas yield, mmol g _{plastic} ⁻¹	66.45	75.77	96.99
Gas yield in relation to plastic only, wt.%	115.39	123.46	144.03
Coke yield in relation to plastic only, wt.%	6.06	5.34	8.49
Gas composition, vol.%			
H ₂	54.58	56.12	59.38
CH ₄	9.83	8.38	6.17
CO	24.17	25.56	26.57
CO ₂	5.92	5.06	5.61
C ₂ -C ₄	5.50	4.89	2.27
H ₂ /CO ratio	2.26	2.20	2.23
Gas yield in relation to plastic & steam, wt.%	28.85	30.86	36.01
Liquid yield in relation to plastic & steam, wt.%	63.74	63.08	60.82
Residue in relation to plastic & steam, wt.%	1.01	0.92	1.18
Mass balance, wt.%	93.60	94.86	98.01

prepared nickel catalyst produced the highest syngas production, while the co-precipitation prepared catalyst produced the lowest syngas production among the three catalysts investigated. In addition, the maximum carbonaceous coke deposition on the catalyst was also obtained with the Ni/Al-Sg catalyst. This suggests that both the hydrocarbon reforming reactions and the hydrocarbon thermal decomposition reactions were promoted more in the presence of the sol-gel prepared catalyst. For example, the largest production of H₂ and CO was obtained with the Ni/Al-Sg catalyst with waste polypropylene at 67.00 mmol H₂ g_{catalyst}⁻¹ and 29.98 mmol CO g_{catalyst}⁻¹ and also the highest coke yield of 8.49 wt.%. This is in agreement with previous results from Efika et al. [39] that a sol-gel prepared NiO/SiO₂ catalyst generated

higher syngas yield than the catalyst made by an incipient wetness method, and the former one also appeared to have more carbon formation on its surface. Although the syngas production achieved the maximum at the presence of Ni/Al-Sg, it should still be noted that the CO content was relatively high. It may be related to the high reforming temperature which was unfavourable to the Reaction (3) due to the exothermic nature of the reaction [40]. Furthermore, a dual functional Ni catalyst with both catalysis and CO₂ sorption, for example, a sol-gel prepared Ni/Al catalyst coupled with CaO, was suggested for further study, in order to promote the WGS reaction for higher H₂ yield [37,41].

The catalytic performance in terms of hydrogen yield and CO production was also influenced by physicochemical characteristics e.g. the porosity, and the type of coke deposited. In particular, the increase in the surface area and pore volume could not only improve the dispersion of metal ions, but also facilitate the interaction of reactant molecules with the catalyst internal surface [42]. In addition, the catalyst was generally deactivated by two types of carbonaceous coke, amorphous (or monoatomic) and filamentous carbon. The filamentous carbon was found to have little influence on the catalytic activities, while the amorphous carbon has been reported to be more detrimental to catalyst activity [13]. Furthermore, these two factors are associated with each other, as Li et al. [43] have suggested that the catalyst activity can be improved by uniform Ni dispersion, while uneven distribution and large Ni particles are the main reason for the formation of non-filamentous coke which leads to the loss of catalyst activity.

In this work, the sol-gel prepared Ni catalyst showed a high surface area and uniform Ni dispersion, as evidenced from the BET and TEM results. Furthermore, the coke obtained is in the filamentous form (from TPO and SEM results). Therefore, the Ni/Al-Sg prepared catalyst presents an excellent catalytic performance towards syngas production for the pyrolysis-catalytic steam reforming of waste plastics. However, for

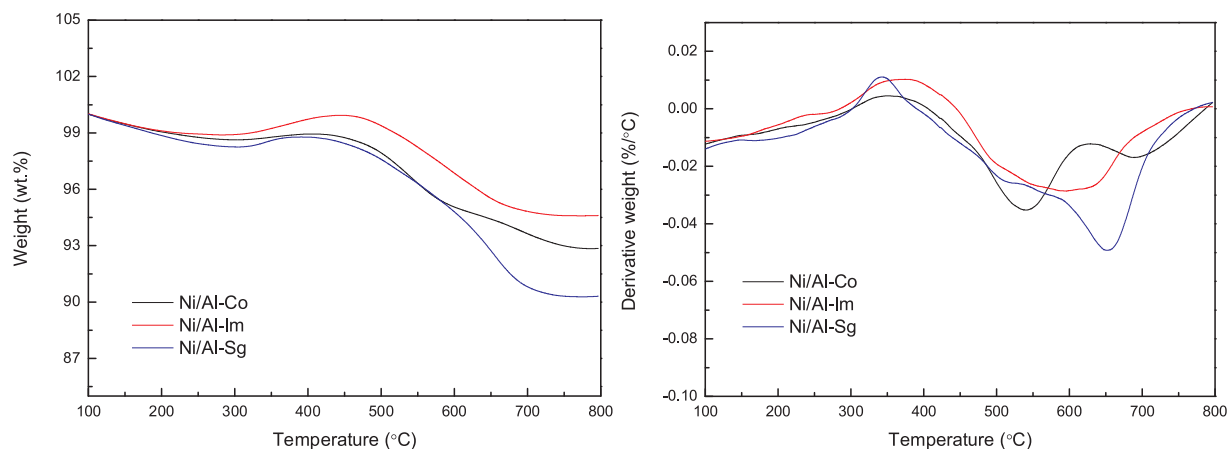


Fig. 9. Temperature programmed oxidation of reacted Ni/Al catalysts for waste polypropylene.

the co-precipitation prepared Ni catalyst, the catalyst coke deposits were found to be of the monoatomic or amorphous type, though it showed a higher surface area than the Ni/Al-Im catalyst. It suggests that a high activity at the initial reaction stage may occur, but it experienced a rapid deactivation by detrimental coke deposition.

4.2. Effect of plastic type on syngas production and coke deposits

The hydrogen and carbon monoxide yield from the pyrolysis-catalytic steam reforming of PP was higher than that observed for HDPE, no matter which catalyst was applied, indicating more syngas production can be obtained per mass of PP compared to HDPE in this work. This may be due to the fact that PP had higher H and C elemental contents compared to HDPE (Table 1), while the ash content of HDPE was

relatively higher. In addition, PS was found to produce the highest CO and syngas yield among the three plastics. Barbarias et al. [44] investigated the valorisation of PP, PE, PS and PET for hydrogen production by pyrolysis-catalytic steam reforming. The pyrolysis volatiles at 500 °C were identified, and results show that nearly 100 wt.% of PS was converted into volatiles with 70.6 wt.% of styrene, while more than 65 wt.% of wax were obtained from polyolefins. Therefore, the higher syngas production from PS in this study may due to the fact that more styrene from PS pyrolysis instead of the wax from polyolefins were introduced into the steam reforming stage. They concluded that the H₂ yields from PS was lower than those from polyolefins, while the H₂ production from PS in this study was comparative even higher than those from HDPE and PP. Around 38, 35 and 30 wt.% of hydrogen yield were achieved by the same authors [44,45] at 16.7 g_{cat} min g_{plastic}⁻¹

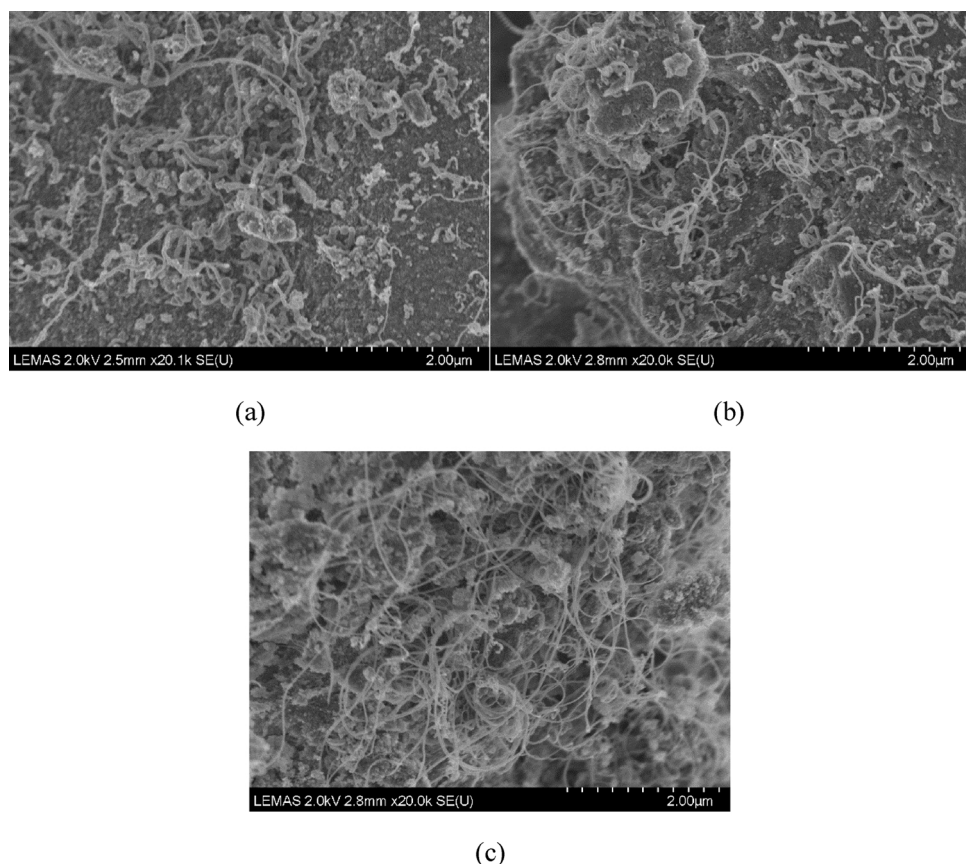


Fig. 10. SEM images of reacted (a) Ni/Al-Co, (b) Ni/Al-Im and (c) Ni/Al-Sg catalyst from waste polypropylene.

Table 5

Gas productions from pyrolysis-catalytic steam reforming of waste polystyrene.

	Ni/Al-Co	Ni/Al-Im	Ni/Al-Sg
H ₂ yield, mmol g _{plastic} ⁻¹	51.31	55.04	62.26
CO yield, mmol g _{plastic} ⁻¹	26.36	30.14	36.10
Syngas yield, mmol g _{plastic} ⁻¹	77.67	85.18	98.36
Gas yield in relation to plastic only, wt.%	116.28	129.08	148.21
Coke yield in relation to plastic only, wt.%	5.64	2.53	6.14
Gas composition, vol.%			
H ₂	59.32	58.39	57.90
CH ₄	2.15	1.79	1.54
CO	30.47	31.97	33.58
CO ₂	6.98	6.79	6.38
C ₂ -C ₄	1.08	1.05	0.60
H ₂ /CO ratio	1.95	1.83	1.72
Gas yield in relation to plastic & steam, wt.%	29.07	32.27	37.05
Liquid yield in relation to plastic & steam, wt.%	67.04	59.43	58.23
Residue in relation to plastic & steam, wt.%	0.71	0.32	0.77
Mass balance, wt.%	96.82	92.02	96.05

space time, 700 °C from HDPE, PP and PS respectively. The difference between those values and the yield in this work were attributed to the different reactor system as well as the operational parameters.

However, in this study, it is still difficult to evaluate the ability of each plastic for H₂ and CO production in relation to C or H elemental content. Therefore, CO conversion Eq. (5) and H₂ conversion Eq. (6) were calculated, to reveal the degree of C or H in the gas product. These two indicators essentially reflect the reforming ability of each plastic by catalyst towards H₂ or CO. In addition, the coke conversion was also calculated as Eq. (7).

$$\text{CO conversion (wt. \%) = (C content in CO gas) / (C content in raw plastic)}$$
 (5)

$$\text{H}_2 \text{ conversion (wt. \%) = (H content in H}_2 \text{ gas) / (H content in raw plastic)}$$
 (6)

$$\text{Coke conversion (wt. \%) = (Coke yield per unit mass of plastic) / (C content in raw plastic)}$$
 (7)

The results of these indicators with the Ni/Al-Sg catalyst was taken as an example in relation to the different plastics and the results presented in Fig. 13 (the results with the other two catalysts are not presented here, but they show a similar trend). From Fig. 13, the ability for H₂ production of HDPE and PP was rather close, as the H₂ conversion obtained was around 95 wt.%. However, the H₂ conversion was significantly increased in the presence of PS, with the highest conversion of 145.11 wt.%. The conversion of over 100 percent was due to the production of H₂ from H₂O. The CO conversion was gradually increased with the order: HDPE < PP < PS and suggests that the steam

reforming reaction of hydrocarbons (Eq. (2)) was more favourable with PS, generating more H₂ and CO. The maximum syngas production of 98.36 mmol g_{plastic}⁻¹ was obtained using PS with the Ni/Al-Sg catalyst. In regard to the gas compositions from different plastics, the molar ratio of H₂/CO achieved was in the range of 1.72 to 2.62, and it was relatively higher from the polyolefin plastics. Therefore, there should be potential in industrial applications in that the H₂ to CO ratio can be tuned to meet the desired ratio by adjusting the mixed proportion of different plastics.

From the TPO results related to catalyst carbon coke deposition, PP generated the highest coke yield of 8.48 wt.%, but from Fig. 13, it can be seen that the calculated carbon conversion was in order of PP > HDPE > PS, even though PS has more C content in the feedstock. The results suggest that the coke formation by decomposition of hydrocarbons Eq. (4) was more favourable in the presence of PP. Wu and Williams [37] also found that PP generated the highest coke deposition on used Ni catalysts when the catalyst temperature was 800 °C with a water flow rate of 4.74 g h⁻¹, compared with HDPE and PS. Also, PS produced relatively lower coke yield among the three plastics under variable process conditions. A similar trend was also reported by Acomb et al. [46], when exploring the pyrolysis-gasification of LDPE, PP and PS, as higher residue yields were obtained from LDPE and PP. Furthermore, the reforming temperature in this work was 800 °C, and Namioka et al. [7] also found that the coke deposition of PP was more apparent than that of PS at higher reforming temperatures (> 903 K).

In relation to the type of carbon deposition on the catalyst, the results show that the carbon was mainly in the form of the filamentous type from waste HDPE and PP (Fig. 7) and Fig. 9), while more amorphous carbon was produced from PS (Fig. 11). This phenomenon was especially evident for the Ni/Al-Im and Ni/Al-Sg catalysts, which generated both types of carbon. This can be explained by the difference in the gas composition, as Angeli et al. [47] suggested that the increase in the C-number in the mixed gases favoured the formation of filamentous carbon, and Ochoa et al. [48] reported that the carbonization of adsorbed coke to form multi-walled filamentous carbon can be promoted by the reaction of CH₄ dehydrogenation. In this work, HDPE and PP produced a higher content of C₁-C₄ hydrocarbon gases compared with PS (comparing Tables 3–5), resulting in the two polyolefin plastics producing more filamentous carbon on the used catalyst.

5. Conclusions

The Ni/Al catalyst prepared by the sol-gel method generated higher H₂ and CO yields from waste plastics than the catalysts prepared by co-precipitation and impregnation, due to the higher surface area and fine nickel particle size with uniform dispersion.

The Ni/Al-Co catalyst prepared by co-precipitation produced the least syngas yield among three catalyst preparation methods

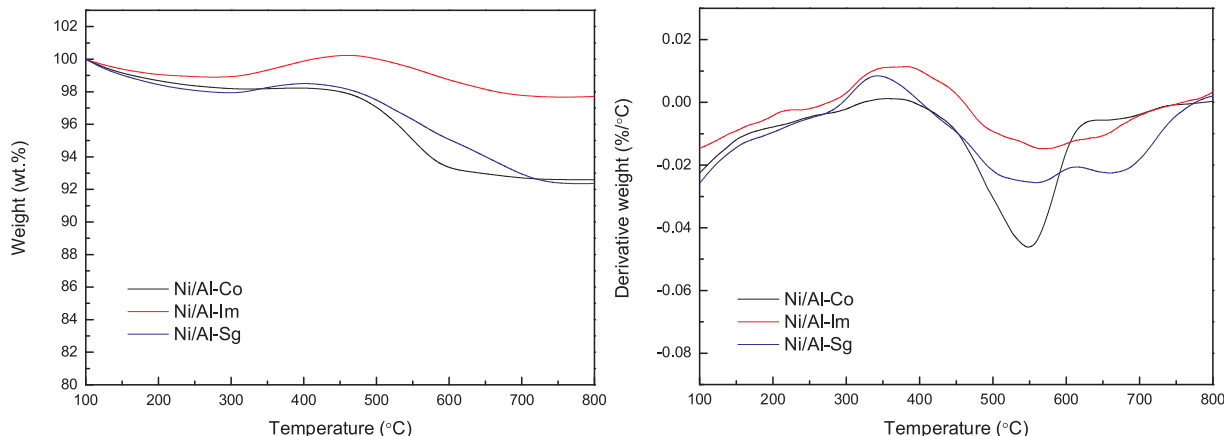


Fig. 11. Temperature programmed oxidation of reacted Ni/Al catalysts for waste polystyrene.

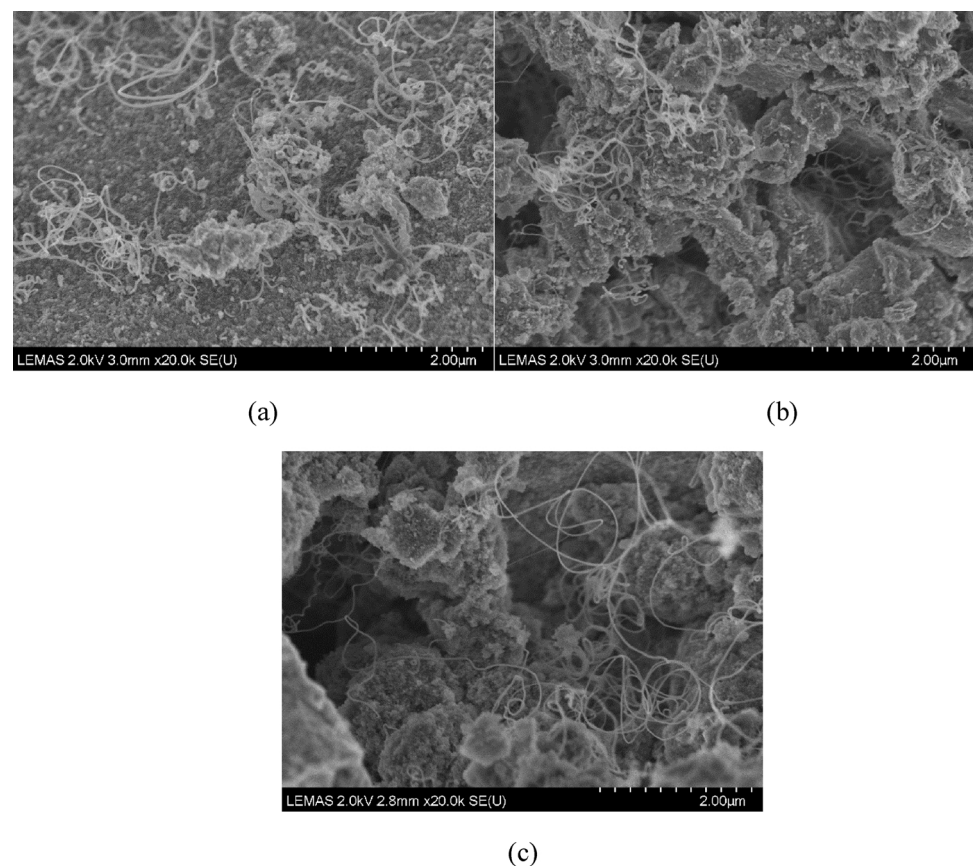


Fig. 12. SEM images of reacted (a) Ni/Al-Co, (b) Ni/Al-Im and (c) Ni/Al-Sg catalyst for waste polystyrene.

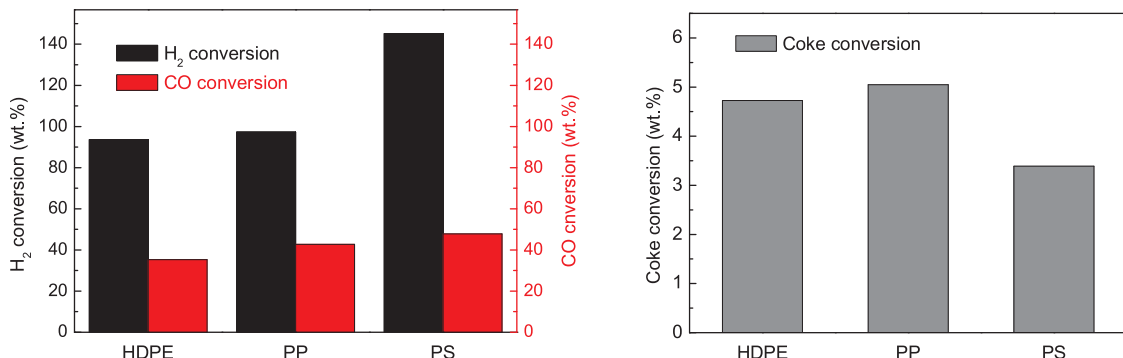


Fig. 13. The conversion of H₂, CO and coke of different plastic with Ni/Al-Sg catalyst.

investigated. From the TPO results, the type of carbon deposited on the Ni/Al-Co catalyst was mainly amorphous type carbon while it was in filamentous form for the impregnation (Ni/Al-Im) and sol-gel (Ni/Al-Sg) prepared catalysts.

Thermal decomposition reactions were more favoured with olefin type plastics (HDPE and PP) to produce higher hydrogen and coke, whereas the steam reforming reactions were more significant with polystyrene. The maximum H₂ yield of 67.00 mmol g⁻¹_{plastic} was obtained from pyrolysis-catalytic steam reforming of waste polypropylene with more hydrocarbons in the product gases, while waste polystyrene generated the highest syngas yield of 98.36 mmol g⁻¹_{plastic} with more oxygen-containing gases in the produced gases.

Acknowledgements

The authors wish to express their sincere thanks for the financial

support from the National Natural Science Foundation of China (51622604) and the Foundation of State Key Laboratory of Coal Combustion (FSKLCCB1805). The experiment was also assisted by the Analysis Laboratory in the School of Chemical and Process Engineering at the University of Leeds and Analytical and Testing Center in Huazhong University of Science & Technology (Wuhan, China). This project has received funding from the European Union's Horizon 2020 research and innovation programme under the Marie Skłodowska-Curie grant agreement No. 643322 (FLEXI-PYROCAT).

References

- [1] S. Wong, N. Ngadi, T. Abdullah, I. Inuwa, Renew. Sustain. Energy Rev. 50 (2015) 1167–1180.
- [2] J.R. Jambeck, R. Geyer, C. Wilcox, T.R. Siegler, M. Perryman, A. Andrady, R. Narayan, K.L. Law, Science 347 (2015) 768–771.
- [3] S.D.A. Sharuddin, F. Abnisa, W.M.A.W. Daud, M.K. Aroua, Energy Convers. Manage

115 (2016) 308–326.

[4] D. Yao, C. Wu, H. Yang, Y. Zhang, M.A. Nahil, Y. Chen, P.T. Williams, H. Chen, Energy Convers. Manag. 148 (2017) 692–700.

[5] C. Wu, P.T. Williams, Int. J. Hydrogen Energy 35 (2010) 949–957.

[6] Y. Park, T. Namioka, S. Sakamoto, T.-j. Min, S.-a. Roh, K. Yoshikawa, Fuel Process. Technol. 91 (2010) 951–957.

[7] T. Namioka, A. Saito, Y. Inoue, Y. Park, T.-j. Min, S.-a. Roh, K. Yoshikawa, ACS Appl. Energy Mater. 88 (2011) 2019–2026.

[8] A. Erkiaga, G. Lopez, I. Barbarias, M. Artetxe, M. Amutio, J. Bilbao, M. Olazar, J. Anal. Appl. Pyrolysis 116 (2015) 34–41.

[9] G. Lopez, A. Erkiaga, M. Artetxe, M. Amutio, J. Bilbao, M. Olazar, Ind. Eng. Chem. Res. 54 (2015) 9536–9544.

[10] G. Lopez, M. Artetxe, M. Amutio, J. Alvarez, J. Bilbao, M. Olazar, Renew. Sustain. Energy Rev. 82 (2018) 576–596.

[11] M.M. Laura, A. Umberto, AIChE J. 54 (2008) 1656–1667.

[12] D. Yao, Y. Zhang, P.T. Williams, H. Yang, H. Chen, Appl. Catal. B-Environ. 221 (2018) 584–597.

[13] C. Wu, P.T. Williams, Appl. Catal. B-Environ. 87 (2009) 152–161.

[14] C. Wu, P.T. Williams, Energy Fuels 22 (2008) 4125–4132.

[15] Y. Shen, P. Zhao, Q. Shao, D. Ma, F. Takahashi, K. Yoshikawa, Appl. Catal. B-Environ. 152 (2014) 140–151.

[16] J. Mazumder, H.I. de Lasa, Appl. Catal. B-Environ. 168 (2015) 250–265.

[17] C. Wu, P.T. Williams, Appl. Catal. B-Environ. 90 (2009) 147–156.

[18] M. Sánchez-Sánchez, R. Navarro, J. Fierro, Int. J. Hydrogen Energy 32 (2007) 1462–1471.

[19] S. Karnjanakom, G. Guan, B. Asep, X. Du, X. Hao, C. Samart, A. Abudula, Energy Convers. Manag. 98 (2015) 359–368.

[20] W. Yang, H. Liu, Y. Li, H. Wu, D. He, Int. J. Hydrogen Energy 41 (2016) 1513–1523.

[21] Y. Bang, S. Park, S.J. Han, J. Yoo, J.H. Song, J.H. Choi, K.H. Kang, I.K. Song, Appl. Catal. B-Environ. 180 (2016) 179–188.

[22] G. Li, L. Hu, J.M. Hill, Appl. Catal. A-Gen. 301 (2006) 16–24.

[23] M.A. Goula, N.D. Charisiou, K.N. Papageridis, A. Delimitis, E. Pachatouridou, E.F. Iliopoulou, Int. J. Hydrogen Energy 40 (2015) 9183–9200.

[24] L. Dong, C. Wu, H. Ling, J. Shi, P.T. Williams, J. Huang, Fuel 188 (2017) 610–620.

[25] F. Chen, C. Wu, L. Dong, A. Vassallo, P.T. Williams, J. Huang, Appl. Catal. B-Environ. 183 (2016) 168–175.

[26] X. Liu, Y. Zhang, M.A. Nahil, P.T. Williams, C. Wu, J. Anal. Appl. Pyrolysis 125 (2017) 32–39.

[27] S.J.H. Rad, M. Haghighi, A.A. Eslami, F. Rahmani, N. Rahemi, Int. J. Hydrogen Energy 41 (2016) 5335–5350.

[28] F. Bimbela, J. Abrego, R. Puerta, L. García, J. Arauzo, Appl. Catal. B-Environ. 209 (2017) 346–357.

[29] M. Sharifi, M. Haghighi, F. Rahmani, S. Karimipour, J. Nat. Gas Sci. Eng. 21 (2014) 993–1004.

[30] C. Wu, P.T. Williams, Environ. Sci. Technol. 44 (2010) 5993–5998.

[31] Y. Xue, P. Johnston, X. Bai, Energy Convers. Manage 142 (2017) 441–451.

[32] I. Barbarias, G. Lopez, M. Amutio, M. Artetxe, J. Alvarez, A. Arregi, J. Bilbao, M. Olazar, Appl. Catal. A-Gen. 527 (2016) 152–160.

[33] D. Yao, H. Yang, H. Chen, P.T. Williams, Appl. Catal. B-Environ. 227 (2018) 477–487.

[34] M. Thommes, K. Kaneko, A.V. Neimark, J.P. Olivier, F. Rodriguez-Reinoso, J. Rouquerol, K.S. Sing, Pure Appl. Chem. 87 (2015) 1051–1069.

[35] D. Yao, C. Wu, H. Yang, Q. Hu, M.A. Nahil, H. Chen, P.T. Williams, Int. J. Hydrogen Energy 39 (2014) 14642–14652.

[36] J.C. Acomb, C. Wu, P.T. Williams, Appl. Catal. B-Environ. 180 (2016) 497–510.

[37] C. Wu, P.T. Williams, Fuel 89 (2010) 3022–3032.

[38] S. Czernik, R.J. French, Energ. Fuel. 20 (2006) 754–758.

[39] C.E. Efika, C. Wu, P.T. Williams, J. Anal. Appl. Pyrolysis 95 (2012) 87–94.

[40] C. Wu, P.T. Williams, Energ. Fuel. 23 (2009) 5055–5061.

[41] F. Jin, H. Sun, C. Wu, H. Ling, Y. Jiang, P.T. Williams, J. Huang, Catal. Today 309 (2018) 2–10.

[42] B.-S. Wang, J.-P. Cao, X.-Y. Zhao, Y. Bian, C. Song, Y.-P. Zhao, X. Fan, X.-Y. Wei, T. Takarada, Fuel Process. Technol. 136 (2015) 17–24.

[43] X. Li, D. Li, H. Tian, L. Zeng, Z.-J. Zhao, J. Gong, Appl. Catal. B-Environ. 202 (2017) 683–694.

[44] I. Barbarias, G. Lopez, M. Artetxe, A. Arregi, J. Bilbao, M. Olazar, Energy Convers. Manage. 156 (2018) 575–584.

[45] I. Barbarias, G. Lopez, J. Alvarez, M. Artetxe, A. Arregi, J. Bilbao, M. Olazar, Chem. Eng. J. 296 (2016) 191–198.

[46] J.C. Acomb, C. Wu, P.T. Williams, Appl. Catal. B-Environ. 147 (2014) 571–584.

[47] S.D. Angelis, F.G. Pilitsis, A.A. Lemonidou, Catal. Today 242 (2015) 119–128.

[48] A. Ochoa, I. Barbarias, M. Artetxe, A.G. Gayubo, M. Olazar, J. Bilbao, P. Castaño, Appl. Catal. B-Environ. 209 (2017) 554–565.